

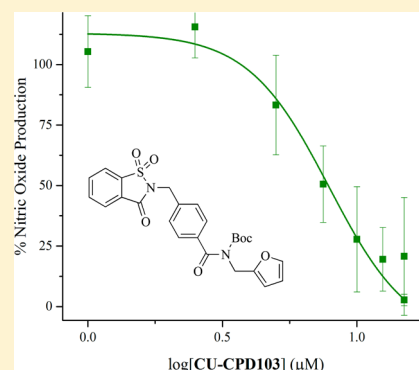
# Saccharin Derivatives as Inhibitors of Interferon-Mediated Inflammation

Adam Csakai,<sup>†</sup> Christina Smith,<sup>†</sup> Emily Davis, Alexander Martinko, Sara Coulup, and Hang Yin\*

Department of Chemistry & Biochemistry and the BioFrontiers Institute, University of Colorado Boulder, 596 UCB, Boulder, Colorado 80309-0596, United States

**S** Supporting Information

**ABSTRACT:** A series of novel, saccharin-based antagonists have been identified for the interferon signaling pathway. Through in vitro high-throughput screening with the Colorado Center for Drug Discovery (C2D2) Pilot Library, we identified hit compound **1**, which was the basis for extensive structure–activity relationship studies. Our efforts produced a lead anti-inflammatory compound, *tert*-butyl *N*-(furan-2-ylmethyl)-*N*-{4-[(1,1,3-trioxo-2,3-dihydro-1 $\lambda$ <sup>6</sup>,2-benzothiazol-2-yl)methyl]benzoyl}-carbamate CU-CPD103 (**103**), as a potent inhibitor using an established nitric oxide (NO) signaling assay. With further studies of its inhibitory mechanisms, we demonstrated that **103** carries out this inhibition through the JAK/STAT1 pathway, providing a drug-like small molecule inflammation suppressant for possible therapeutic uses.



## INTRODUCTION

Interferons (IFN) are a linchpin of inflammatory signaling, assisting in host defense against pathogens, antigen presentation, and immunomodulation. There are two main classes of interferons: type I (IFN- $\alpha/\beta$ ) and type II (IFN- $\gamma$ ).<sup>1</sup> Interferons bind to their respective transmembrane receptors, inducing dimerization and regulation of inflammatory gene expression through the JAK/STAT signaling pathway.<sup>1</sup> Janus kinases (JAKs) are tyrosine kinases that interact with interferon receptors, resulting in recruitment and phosphorylation of signal transduction and activator of transcription (STAT) proteins.<sup>2</sup> The JAK/STAT association in turn promotes transcription of pro-inflammatory genes including inducible nitric oxide synthase (iNOS).<sup>3</sup>

Interferons coordinate the inflammation response in concert with other innate immune pathways, particularly Toll-like receptor (TLR) signaling. TLRs are pattern recognition receptors that respond to infectious markers and induce a pro-inflammatory response.<sup>4,5</sup> These two pathways synergistically interact in macrophages to elicit an immune response toward infective threats. Macrophage priming with IFN- $\gamma$  improves the inflammatory response to TLR ligands, such as lipopolysaccharide (LPS) for TLR4. In turn, TLRs upregulate type I interferons, and NF- $\kappa$ B assists in transcription of multiple interferon-inducible genes.<sup>6</sup> Of particular interest, the iNOS promoter has binding sites for both STAT1 and NF- $\kappa$ B.<sup>7</sup> Transcription of iNOS may be activated by multiple inflammatory factors, including LPS, type I, and type II interferons.<sup>8</sup> STAT1 activation by IFN- $\beta$  has an autocrine/paracrine mechanism preceding iNOS activation and serves as a necessary transcription factor for synthesis.<sup>9</sup> It has been demonstrated that knockdown of the interferon- $\alpha/\beta$  receptor

1 (IFNAR1) mitigates iNOS expression, even in the presence of LPS.<sup>10</sup> IFN- $\gamma$  activates STAT1 through interaction with its cognate receptor IFNGR, upregulating iNOS.<sup>11</sup> Thus, activation of the TLR and interferon interrelated pathways can be regulated at their convergence in JAK/STAT signaling. Nonetheless, it has been a significant challenge to regulate individual pathways with high specificity and selectivity.

Generally, inflammatory signaling is beneficial and may protect the host against infection. However, in autoimmune pathologies such as systemic lupus erythematosus and multiple sclerosis, an overabundance of interferon signaling can have deleterious effects.<sup>12–14</sup> Indeed, it has been noted that among centenarian women, polymorphisms that result in decreased IFN- $\gamma$  may contribute to longevity.<sup>15</sup> Additionally, a small molecule modulator of IFN signaling may provide a useful tool in the study and treatment of autoimmune diseases. Here, we report a small molecule that is able to inhibit the interferon-induced JAK/STAT1 signaling pathway without compromising the effectiveness of other components of the innate immune system such as TLRs.

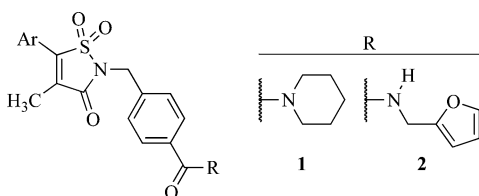
## RESULTS AND DISCUSSION

**C2D2 Compound Library Screening.** We started our search for anti-inflammatory agents by looking for inhibitors of LPS-induced TLR4 activation. The Colorado Center for Drug Discovery (C2D2) compound library was screened.<sup>16</sup> The C2D2 pilot library consists of 2200 drug-like compounds that represent a variety of diverse and commercially available scaffolds. The initial screen was performed using LPS-activated

Received: March 17, 2014

Published: May 24, 2014

RAW 264.7 cells in a 96-well plate format to monitor nitric oxide (NO) production. This assay uses a Sandmeyer reaction to convert 2,3-diaminonaphthalene to fluorescent naphthalene-triazole in the presence of NO. As NO is produced in the TLR inflammatory response, this readout provides information on the extent of TLR signaling. Initial screening yielded 31 hits, representing 5 scaffolds (Figure S1, Supporting Information). We selected the scaffold with an isothiazolone 1,1-dioxide core for further development as it produced the most numerous and potent hits. Compounds **1** and **2** (Figure 1) represent two of the more potent hits.



**Figure 1.** Generic scaffold of hit molecules selected from the screening of the Colorado Center for Drug Discovery (C2D2) Pilot Library. Both variable functionalities (Ar = substituted benzene ring, R = various amide moieties) shown in these representative structures have been subsequently optimized.

### Synthesis and Structure–Activity Relationship (SAR).

We have developed an efficient synthetic route for the generic scaffold in Figure 1. As an example, the synthesis of the most potent hit molecule, **1** (Scheme 1), began with the oxidative dimerization of commercially available **3** to give dithiodipropionic acid **4**.<sup>17</sup> Conversion to the dithiodipropionyl chloride was completed with thionyl chloride, and subsequent treatment with anhydrous ammonia gave dithiodipropionamide **5** as a mixture of diastereomers.<sup>17</sup> As previously described by Lewis and co-workers, oxidative cyclization was performed with sulfuric acid to give an inseparable mixture of **6** and **7**.<sup>17</sup> This mixture of isothiazolinones was then deprotonated with sodium hydride, and alkylated with benzyl chloride **9**. The alkylation yields two synthetically useful intermediates **12** and **13**, which are easily separable by column chromatography. Chloro-intermediate **12** was oxidized with *meta*-chloroperoxybenzoic acid (*m*-CPBA) to give the isothiazolone 1,1-dioxide core, **14**.

Chloro-intermediate **14** was coupled to 3,4-dimethylphenylboronic acid, using previously reported conditions to give the parent library hit, **1**.<sup>18</sup> Identical conditions were used to synthesize a related  $\beta$ -naphthalene analogue, **15**. These conditions failed, however, when 4-pyridinylboronic acid was used. Making use of intermediate **13** with Heck conditions and 4-bromopyridine-HCl successfully gave **16**. The coupling product **16** was fully oxidized at both sulfur and the pyridyl nitrogen to give **17**. The synthesis of compounds **15** and **17** provide analogues that exhibit both higher and lower calculated log *P* values, 4.70 and 1.29 respectively, as compared to **1** (4.46). However, **15** only showed a small improvement in potency, and **17** showed greatly reduced potency as compared to **1** (Table 1).

The 2-benzyl-4-methyl-5-phenylisothiazol-3-one 1,1-dioxide core of **1**, **15**, and **17** was sensitive to a variety of mild reaction conditions. We commonly observed complex mixtures in efforts to synthesize other analogues. The few successfully synthesized analogues exhibited only modest activity, so we thought it best to make more drastic structural changes. In an effort to simplify

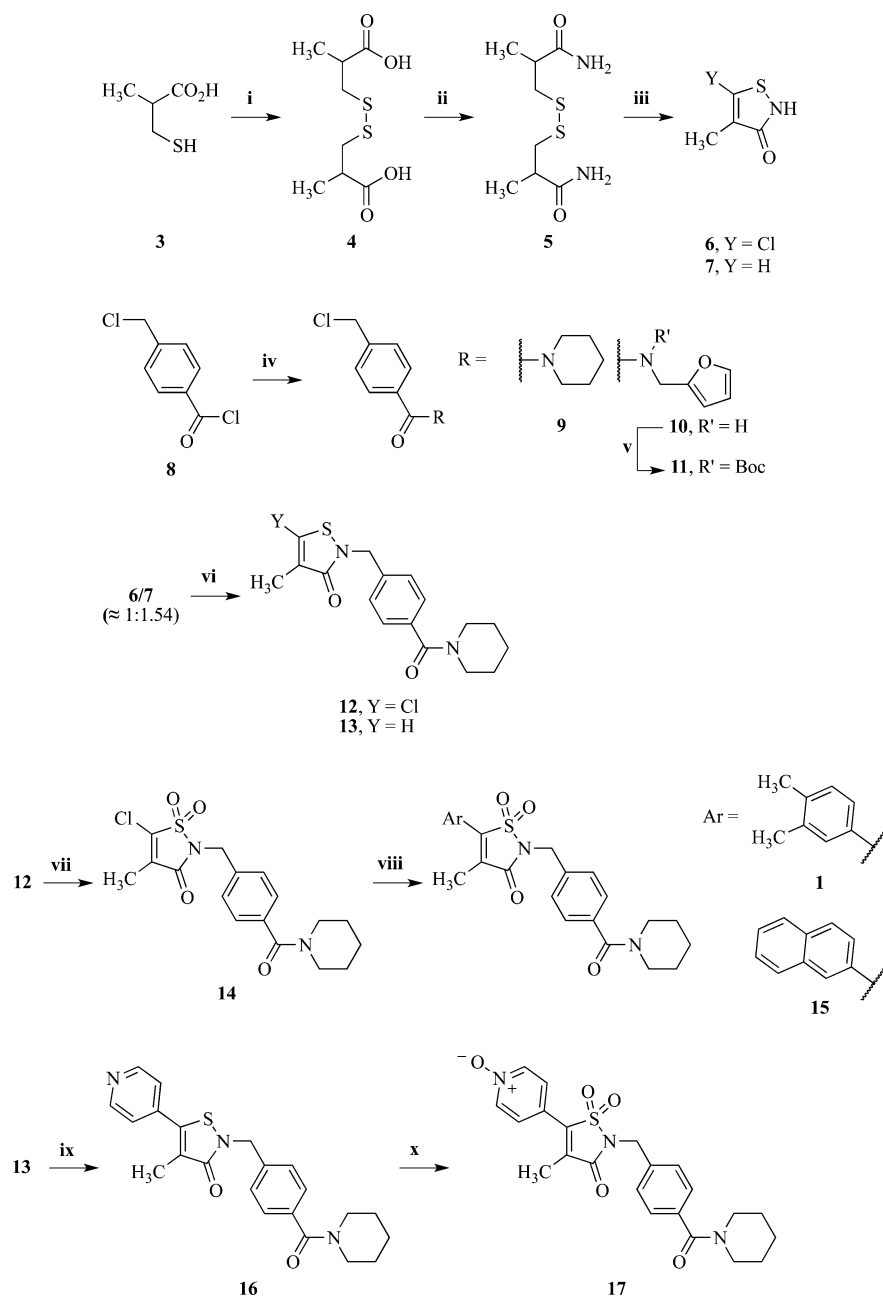
synthesis and increase stability, we took inspiration from saccharin **18** (Scheme 2).

Saccharin inspired analogues, **19** and CU-CPD103 (**103**), were easily synthesized from commercially available saccharin and previously synthesized benzyl chlorides **9** and **11**. **103** is easily deprotected with TFA to give **20**. A significant improvement in activity was observed with intermediate **103**, so we sought related analogues **26–43** (Scheme 3; detailed syntheses can be found in the Supporting Information). Compounds **19**, **20**, **103**, and **26–43** contain the same piperidine or furfuryl amide moieties (Figure 1) that were present in our initial library screen so we could have a consistent basis for comparison. The lithium aluminum hydride reduction of saccharin **18**, previously described by Porter and co-workers,<sup>19</sup> provided 2,3-dihydro-1,1-dioxo-1,2-benzisothiazole **21**. Alkylation of this sultam with **9** and **11** provided analogues **26** and **27**. Commercially available 1-isindolinone **22**, phthalimide potassium salt **23**, 1,2-benzisothiazol-3(2*H*)-one **24**, and 3-hydroxybenzisoxazole **25**, were alkylated with **9** and **11** to give analogues **29**, **30**, **32**, **33**, **35**, **36**, **38**, and **39** (Scheme 3). Treatment of analogues **35** and **36** with *m*-CPBA at 0 °C gave analogues **38** and **39**, respectively, as racemic mixtures. All Boc protected analogues were treated with trifluoroacetic acid in methylene chloride to give deprotected analogues **28**, **31**, **34**, **37**, **40**, and **43**.

The removal of the saccharin series 3-position carbonyl gave us the sultam series **26**, **27**, and **28** (Table 2). As we had seen with the parent saccharin series, the Boc protected amide **27** was the most potent of the series. **27**, however, was unable to match the potency of **103**. For this reason, we believe the 3-position carbonyl to be somewhat important to either binding or cell permeability. Replacement of the saccharin series 1-position SO<sub>2</sub> moiety with a methylene unit gave us the isoindolinone series **29**, **30**, and **31**. Unlike others, the analogue bearing a Boc protected amide **30** shows the lowest potency. All isoindolinone analogues, however, are poor inhibitors. This led us to believe that the 1-position SO<sub>2</sub> moiety makes a significant interaction, perhaps as a hydrogen bond acceptor. As previously discussed, the 3-position carbonyl of **103** appears less significant, so the carbonyl of the isoindolinone **30** may be making a weaker hydrogen bond interaction as a poor bioisostere of the SO<sub>2</sub> moiety. Otherwise, the isoindolinone series would likely have even lower potency.

To further investigate the role of the SO<sub>2</sub> moiety, the 3-position carbonyl of **103** was maintained and the SO<sub>2</sub> moiety replaced with an additional carbonyl, as shown with the phthalimide analogues **32**, **33**, and **34**. The activity of **103** is nearly equal with **33**. As with the parent saccharin analogues, **32** and **34** show little or no activity. This suggests that a carbonyl is a suitable bioisostere to the SO<sub>2</sub> moiety so long as the 3-position carbonyl is intact, unlike **30**.

Furthermore, a loss of one, or both, oxygen atoms from the SO<sub>2</sub> moiety of **103** results in a complete loss of activity, as seen with **36** and **39**. As seen before, the deprotected species **37** and **40** show poor activity. As expected, the piperidine amide analogue, **38** shows a further decrease in potency. However, **35** inexplicably shows comparable potency as compared to **103** and is a great improvement over the related analogue **26**. When the unoxidized sulfur of **36** is replaced with a smaller oxygen atom **42**, the activity is once again comparable to that of **103**. Again, the deprotected analogue **43** shows significantly lower activity, although **41** shows some modest activity.

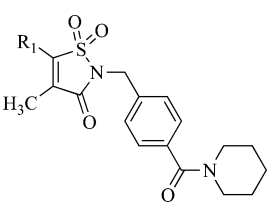
Scheme 1. Isothiazolinone Synthesis<sup>a</sup>

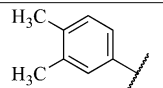
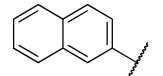
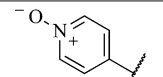
<sup>a</sup>(i) I<sub>2</sub>, KI, NaOH, H<sub>2</sub>O, (4 = 99%); (ii) (1) SOCl<sub>2</sub>, (2) NH<sub>3</sub>, CH<sub>2</sub>Cl<sub>2</sub> (5 = 66%); (iii) SO<sub>2</sub>Cl<sub>2</sub>, EtOAc (6 and 7 = 51%); (iv) piperidine or furfurylamine, DIPEA, CH<sub>2</sub>Cl<sub>2</sub> (9 = 95%, 10 = 99%); (v) Boc<sub>2</sub>O, DMAP, THF (11 = 81%); (vi) (1) NaH, DMF, (2) 9 (12 = 70%, 13 = 67%); (vii) *m*-CPBA, CH<sub>2</sub>Cl<sub>2</sub> (14 = 49%); (viii) ArB(OH)<sub>2</sub>, Pd(dppf)Cl<sub>2</sub>·CH<sub>2</sub>Cl<sub>2</sub>, K<sub>2</sub>CO<sub>3</sub>, 1,4-dioxane (1 = 47%, 15 = 32%); (ix) 4-bromopyridine·HCl, Pd(OAc)<sub>2</sub>, KOAc, DMA (16 = 54%); (x) *m*-CPBA, CH<sub>2</sub>Cl<sub>2</sub> (17 = 84%).

We further investigated the role of the SO<sub>2</sub> moiety by synthesizing the fully reduced and partially reduced variants, 35–40. If the SO<sub>2</sub> moiety does play the role of hydrogen bond acceptor, then these reduced analogues would be less efficacious. As expected, we observed either a loss in activity or no change in activity from analogues 36–40. The fully reduced analogue 35, however, inexplicably shows activity comparable to that of 103. We also synthesized 41–43 as smaller, more basic bioisosteres of 35–37. This modification resulted with a drop in activity for 41 as compared to 35 and a great improvement with 42 as compared to 36. In fact, the potency of 42 is comparable to that of 103, 27, and 33. This

suggests that an oxygen hydrogen bond acceptor is important to activity. The steric constraints of this position seem flexible, given two of the more active analogues in this series, 103 and 42, are the largest and smallest of the series, respectively. The less active of this series are of varying size, but are consistently less basic than the more active analogues.

From this series of molecules, there are five analogues that have IC<sub>50</sub> values of less than or roughly equal to 10 μM. Four of these five analogues have the same Boc-protected furfurylamine (103, 27, 33, and 42). All four of these analogues lose significant activity when deprotected. This implies that there is an important interaction(s) being made with the Boc group,

**Table 1. SAR Summary and Toxicity of 4-Aryl-3-methylisothiazolone 1,1-dioxide Analogues<sup>a</sup>**


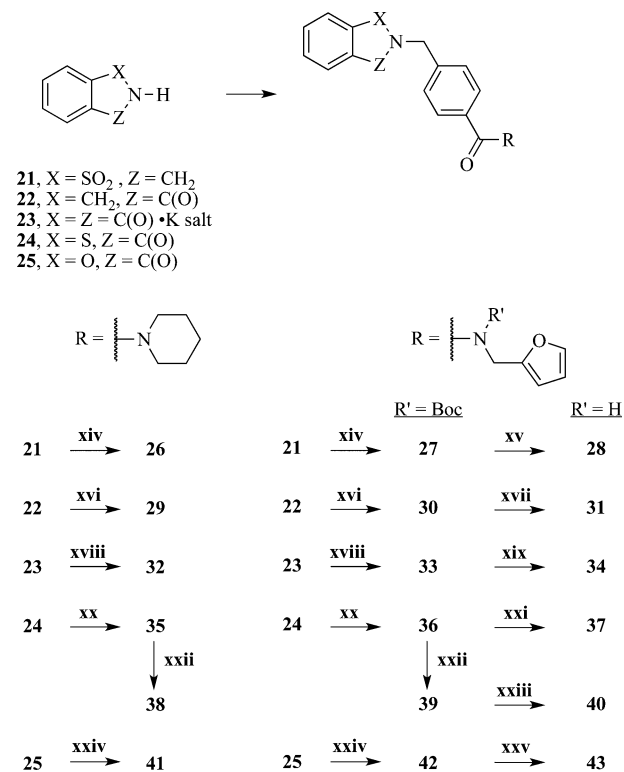
R <sub>1</sub>	ID # Key: IC <sub>50</sub> LC <sub>50</sub>
	<b>1</b> 16.5 ± 0.55 μM >100 μM
	<b>15</b> 9.61 ± 2.56 μM 47.9 ± 5.79 μM
	<b>17</b> 79.4 ± 13.6 μM > 100 μM

<sup>a</sup>Summary of IC<sub>50</sub> values and toxicity for structure–activity relationship studies. IC<sub>50</sub> values were obtained using RAW 264.7 cells treated with 20 ng/mL LPS and varying concentrations of compound. A cell viability assay was used to determine cytotoxicity at each tested concentration. LC<sub>50</sub> is the concentration at which cytotoxicity results in 50% cell viability. The purity of tested compounds was evaluated via <sup>1</sup>H NMR (>95% sample purity).

and/or that an amide N–H causes a deleterious interaction. To better understand this observation, analogues **50**, **52**, **54**, **55**, **56**, **57**, and **58** were synthesized from the corresponding carboxylic acid **45** (Scheme 4).<sup>20</sup>

Interestingly, intermediate ester **44** showed modest activity (Table 3) while intermediate carboxylic acid **45** shows no activity. This may imply that the previously successful analogues bearing Boc groups might be benefiting from hydrophobic interactions with the tertiary butyl moiety. Boc protected amides **52** and **56**, however, have shown very poor activity. Initial efforts to synthesize **56** produced the double-Boc protected amide **50**, which also has poor activity, suggesting that the furan substituent was necessary. We also investigated a very minor change by synthesizing the extended linker analogue **54**. Surprisingly, a significant loss in activity was observed.

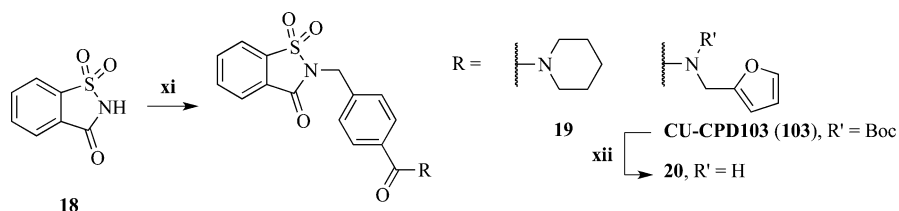
To test if the presence of an acidic amide N–H could be causing a negative effect on activity, we synthesized **55**. However, we observed significantly lower potency, perhaps suggesting that the rotational constraints of a tertiary amide are not conducive to activity. Given this observation, we speculated that perhaps a carbonyl component was still required for

**Scheme 3. Fused Ring Analogues<sup>a</sup>**

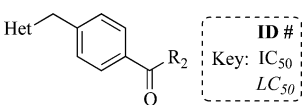
<sup>a</sup>(xiv) (1) NaH, DMF, (2) **9** (**26** = 84%) or **11** (**27** = 81%); (xv) TFA, CH<sub>2</sub>Cl<sub>2</sub> (**28** = 92%); (xvi) (1) NaH, DMF, (2) **9** (**29** = 57%) or **11** (**30** = 10%); (xvii) TFA, CH<sub>2</sub>Cl<sub>2</sub> (**31** = 71%); (xviii) 18-crown-6, DMF, **9** (**32** = 84%) or **11** (**33** = 81%); (xix) TFA, CH<sub>2</sub>Cl<sub>2</sub> (**34** = 81%); (xx) (1) NaH, DMF, (2) **9** (**35** = 48%) or **11** (**36** = 27%); (xxi) TFA, CH<sub>2</sub>Cl<sub>2</sub> (**37** = 97%); (xxii) *m*-CPBA, CH<sub>2</sub>Cl<sub>2</sub>, **35** (**38** = 85%) or **36** (**39** = 79%); (xxiii) TFA, CH<sub>2</sub>Cl<sub>2</sub> (**40** = 92%); (xxiv) (1) NaH, DMF, (2) **9** (**41** = 55%) or **11** (**42** = 14%); (xxv) TFA, CH<sub>2</sub>Cl<sub>2</sub> (**43** = 87%).

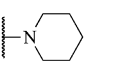
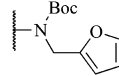
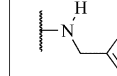
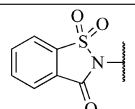
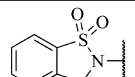
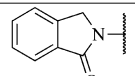
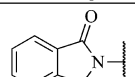
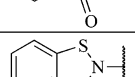
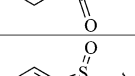
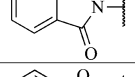
activity. However, the *N*-methylcarbamate and *N*-acyl analogues, **57** and **58**, were significantly less potent than even **20**. We concluded that the furfurylamide component was essential, and that Boc protection was the optimal substituent. On the basis of these results, **103** was selected as our lead compound.

**Anti-Inflammatory Mechanism Studies of 103.** Our initial screen identified compounds that could inhibit the LPS-induced inflammatory response. To determine if **103** specifically targets TLRs, NO signaling was assessed with three different TLR ligands. LPS (TLR4), Poly I:C (TLR3), and Pam<sub>2</sub>CSK<sub>4</sub> (TLR2/6) were chosen to encompass the most variety in signaling, including differences in TLR localization and adaptor proteins (Figure S3, Supporting Information). As Figure 2 shows, **103** inhibits NO signaling regardless of ligand

**Scheme 2. Saccharin Derived Analogues<sup>a</sup>**

<sup>a</sup>(xi) (1) NaH, DMF, (2) **9** (**19** = 65%) or **11** (**103** = 62%); (xii) TFA, CH<sub>2</sub>Cl<sub>2</sub> (**20** = 87%).

**Table 2. SAR Summary and Toxicity of Saccharin Inspired Analogues<sup>a</sup>**


Het			
	<b>19</b> 50.6 ± 8.48 μM 69.2 ± 1.01 μM	<b>103</b> 2.61 ± 0.40 μM > 100 μM	<b>20</b> 24.3 ± 1.87 μM > 100 μM
	<b>26</b> 44.3 ± 3.72 μM > 100 μM	<b>27</b> 10.6 ± 2.44 μM > 100 μM	<b>28</b> 68.4 ± 24.25 μM > 100 μM
	<b>29</b> 21.9 ± 2.41 μM > 100 μM	<b>30</b> 51.8 ± 6.71 μM 95.2 ± 10.9	<b>31</b> 49.7 ± 24.3 μM > 100 μM
	<b>32</b> >100 μM > 100 μM	<b>33</b> 3.45 ± 1.93 μM > 100 μM	<b>34</b> 56.0 ± 5.85 μM > 100 μM
	<b>35</b> 5.38 ± 1.60 μM 70.3 ± 8.89 μM	<b>36</b> 68.0 ± 30.5 μM > 100 μM	<b>37</b> 19.8 ± 1.72 μM > 100 μM
	<b>38</b> 49.0 ± 4.68 μM > 100 μM	<b>39</b> 68.0 ± 7.83 μM 87.3 ± 6.78 μM	<b>40</b> 23.3 ± 0.68 μM > 100 μM
	<b>41</b> 16.8 ± 5.93 μM 66.2 ± 4.18 μM	<b>42</b> 6.69 ± 1.70 μM > 100 μM	<b>43</b> 49.3 ± 7.02 μM > 100 μM

<sup>a</sup>Summary of IC<sub>50</sub> values and toxicity for structure activity relationship studies. IC<sub>50</sub> values were obtained using RAW 264.7 cells treated with 20 ng/mL LPS and varying concentrations of compound. A cell viability assay was used to determine cytotoxicity at each tested concentration. LC<sub>50</sub> is the concentration at which cytotoxicity results in 50% cell viability. The purity of tested compounds was evaluated via <sup>1</sup>H NMR (>95% sample purity).

treatment. This suggests that **103** does not bind specifically to an individual TLR but rather inhibits a common downstream factor of these TLRs. The dose–response curves for all three ligands show comparable inhibition, with minor deviations due to TLR expression levels and the effectiveness of the ligand to induce inflammation. Primary macrophage cells demonstrated the same behavior as RAW 264.7 cells, with **103** inhibiting LPS signaling with an IC<sub>50</sub> value of 9.61 ± 1.45 μM (Figure S2, Supporting Information). It is important to note that **103** shows no cytotoxicity at concentrations up to 100 μM (Figure S4, Supporting Information).

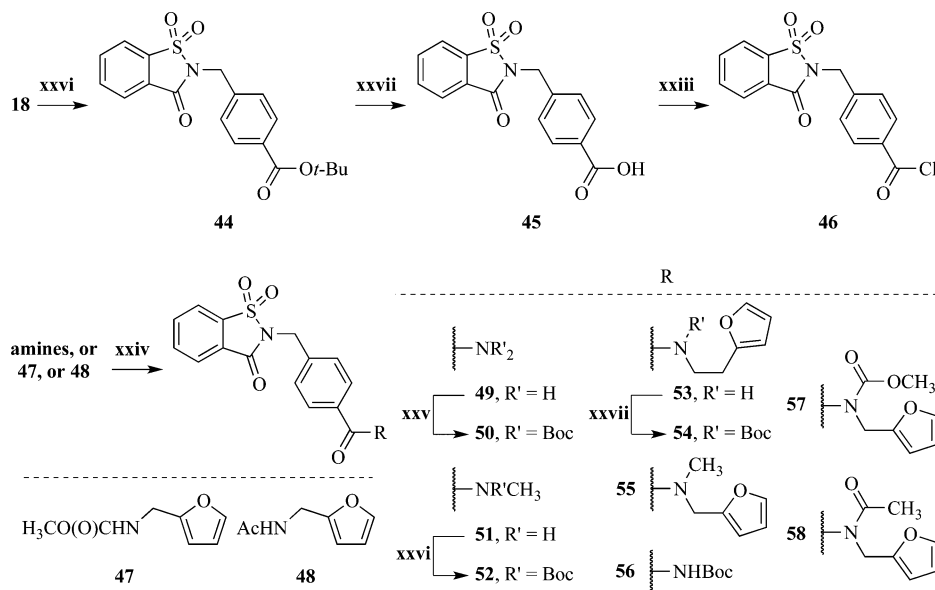
To further confirm that iNOS was being down regulated by treatment with **103**, quantitative real-time polymerase chain reaction (RT-PCR) and Western blot experiments were performed. RT-PCR data was obtained using RAW 264.7 cells treated with LPS and varying concentrations of **103**. Figure 3 demonstrates that treatment with **103** decreases iNOS mRNA in a dose-dependent fashion. Western blots were performed with a pan NOS antibody and again iNOS is seen to decrease in a dose-dependent fashion (Figure 4), indicating that **103** suppresses iNOS at mRNA, protein, and cell signaling levels. While LPS was used as the inflammation-inducing ligand

in the NO production assay to maintain consistency, its effects are indirect. Therefore, a secondary assay that monitors IFN-γ induced mRNA changes was carried out to confirm the validity of the NO assay as the primary readout for understanding SAR and compound optimization (Figure S7, Supporting Information). These results demonstrated the same trend of inhibition for **103**, **36**, and **49** (**49** is commercially available from Enamine Ltd.). Compound **103** is able to inhibit greater than 70% of IFN-γ induced mRNA, whereas **36** and **49** show a weaker potency, with maximum inhibition of 50%. Importantly, these results corroborate the IC<sub>50</sub> values determined in the previously described NO production assay.

Regardless of their ligand or localization, all TLRs activate NF-κB (Figure S3, Supporting Information). To test the inhibitory effects of **103** on NF-κB activity, a secreted embryonic alkaline phosphatase (SEAP) assay was performed in HEK 293T cells. When tested at concentrations up to 100 μM, the compound did not down-regulate NF-κB activation through TLR3 or TLR4 (Figure S5, Supporting Information). To determine if any modulation occurs through other NF-κB pathways, TNF-α was used to activate NF-κB signaling. As seen in the Figure S4 in the Supporting Information, NF-κB signaling through tumor necrosis factor receptor (TNFR) is also unaffected. This data suggests that **103** does not directly modulate the TLR signaling pathway at any point, as NF-κB is essential to all TLR signaling. We next sought to confirm this result through observation of NF-κB-induced cytokines, particularly TNF-α. A commercially available enzyme-linked immunosorbent assay (ELISA) was used to measure TNF-α in RAW 264.7 cells. Figure S6 in the Supporting Information shows that there was no change in TNF-α cytokine levels with compound treatment. These results confirm in two cell types that there is no modulation of NF-κB by **103**, regardless of ligand or signaling pathway. However, previous results demonstrated that TLR-induced NO activation is inhibited by **103**. The iNOS promoter has binding sites for both NF-κB and STAT1. Because NF-κB activation is not being affected with **103** treatment, the inhibition of iNOS was therefore likely to occur within the JAK/STAT1 pathway.

As no direct antagonism was observed through TLRs and NF-κB, additional tests were carried out to identify the potential anti-inflammatory mechanism of **103**. The interferon I (IFN-α/β) and interferon II (IFN-γ) pathways cause upregulation of iNOS, which results in production of NO. As such, we speculated that observed NO inhibition might occur through inhibition of the JAK/STAT signaling pathway. To test this hypothesis, IFN-γ was used as a ligand to activate iNOS in RAW 264.7 cells. Inhibition of NO occurred in a dose-dependent fashion with treatment of **103**. The IC<sub>50</sub> value with IFN-γ is 7.88 ± 1.25 μM, which corroborates the IC<sub>50</sub> value of LPS (Figure 5). This indicated that the JAK/STAT1 pathway is involved in the inhibitory function of **103**. Additionally, as TLR activation results in production of type I interferons, synonymous inhibition with IFN-γ proposes a shared target between these two pathways. Thus, it is likely that the molecular target of **103** lies in the interferon-induced STAT1 pathway.

Additionally, a commercial JAK/STAT RT-PCR array was used to determine if JAK/STAT pathway signaling is by and large modulated with **103** treatment. A summary of the results is available in Supporting Information Table S1. The modified genes, including NOS2, Cebpb, and Gtp1, suggest that **103** modulates STAT1 signaling.<sup>3,21,22</sup> Additional validation is

Scheme 4. Amide Modifications<sup>a</sup>

<sup>a</sup>(xxvi) (1) NaH, DMF, (2) 4-bromomethylbenzoic acid *tert*-butyl ester (**44** = 62%). (xxvii) TFA, CH<sub>2</sub>Cl<sub>2</sub> (**45** = 98%). (xxiii) SOCl<sub>2</sub> (>99%). (xxiv) procedure A, **46** in CH<sub>2</sub>Cl<sub>2</sub>, then ammonia in THF (**49** = 92%), or methylamine in THF (**51** = 79%), or 2-furan-2-yl-ethylamine and DIPEA (**53** = 85%), or *N*-methylfurfurylamine and DIPEA (**55** = 86%); procedure B, (1) *tert*-butylcarbamate, LiHMDS, THF, (2) **46** in CH<sub>2</sub>Cl<sub>2</sub>; procedure C, (1) NaH in DMF, then **47** or **48**, (2) **46** in CH<sub>2</sub>Cl<sub>2</sub> (**57** = 41%, **58** = 17%). (xxv) Boc<sub>2</sub>O, DMAP, CH<sub>2</sub>Cl<sub>2</sub> (**50** = 73%). (xxvi) Boc<sub>2</sub>O, DMAP, CH<sub>2</sub>Cl<sub>2</sub> (**52** = 81%). (xxvii) Boc<sub>2</sub>O, DMAP, CH<sub>2</sub>Cl<sub>2</sub> (**54** = 33%).

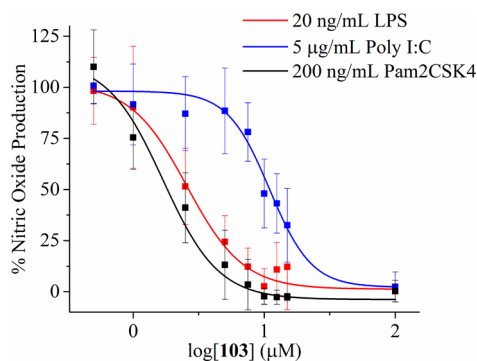
Table 3. SAR Summary and Toxicity of Saccharin Derived Analogues<sup>a</sup>

R <sub>3</sub>	ID # Key: IC <sub>50</sub> LC <sub>50</sub>	R <sub>3</sub>	ID # Key: IC <sub>50</sub> LC <sub>50</sub>
	<b>44</b> 10.6 ± 2.44 μM > 100 μM		<b>52</b> 42.0 ± 3.20 μM > 100 μM
	<b>45</b> 74.7 ± 9.92 μM > 100 μM		<b>53</b> 76.6 ± 6.49 μM > 100 μM
	<b>49</b> 50.6 ± 10.3 μM > 100 μM		<b>54</b> 48.6 ± 7.15 μM > 100 μM
	<b>56</b> 64.7 ± 8.30 μM > 100 μM		<b>55</b> 79.6 ± 3.69 μM > 100 μM
	<b>50</b> 33.4 ± 3.31 μM > 100 μM		<b>57</b> 76.0 ± 8.20 μM > 100 μM
	<b>51</b> 37.7 ± 1.21 μM > 100 μM		<b>58</b> 42.6 ± 5.19 μM > 100 μM

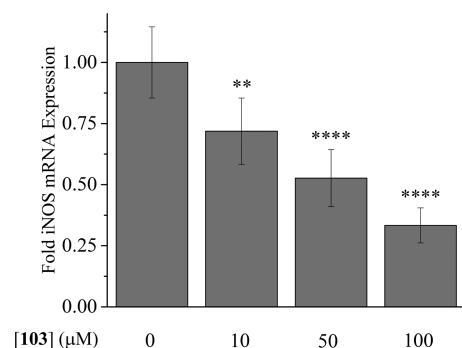
**103**  
2.61 ± 0.40 μM  
> 100 μM

R<sub>3</sub> =

<sup>a</sup>Summary of IC<sub>50</sub> values and toxicity for structure activity relationship studies. IC<sub>50</sub> values were obtained using RAW 264.7 cells treated with 20 ng/mL LPS and varying concentrations of compound. A cell viability assay was used to determine cytotoxicity at each tested concentration. LC<sub>50</sub> is the concentration at which cytotoxicity results in 50% cell viability. The purity of tested compounds was evaluated via <sup>1</sup>H NMR (>95% sample purity).



**Figure 2.** **103** inhibits NO signaling mediated by different TLRs with comparable  $IC_{50}$ s. RAW 264.7 cells were treated with LPS (TLR4 ligand), Poly I:C (TLR3 ligand), or Pam2CSK4 (TLR2/6 ligand). The  $IC_{50}$  values are  $2.61 \pm 0.40$ ,  $10.9 \pm 0.74$ , and  $1.69 \pm 0.43 \mu M$ , respectively. Treatment with **103** decreased NO production with all TLR ligands in a dose-dependent fashion. These results demonstrate that **103** does not specifically inhibit a particular TLR but rather, a common downstream effector. Data was normalized [(raw data-untreated cells)/(TLR agonist + solvent control-untreated cells)] such that TLR agonist + solvent is 100% activation, and untreated cells are 0% activation. Data points shown are the average of nine replicates, with error bars represented as the standard deviation.

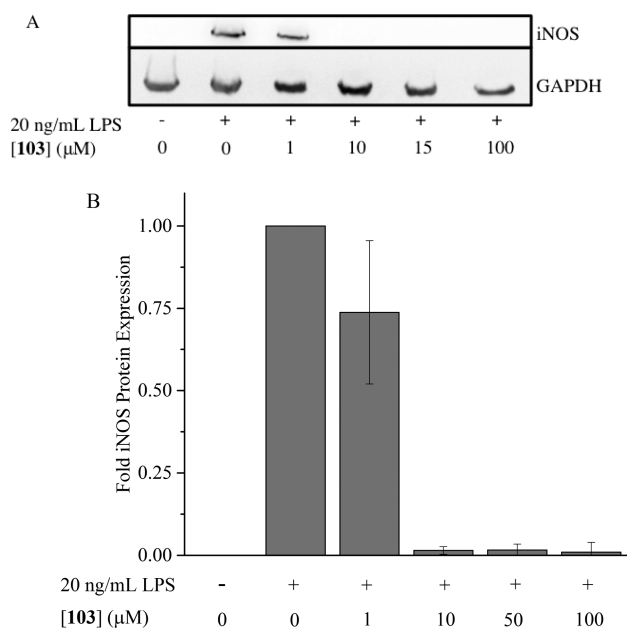


**Figure 3.** **103** treatment decreases iNOS mRNA in a dose-dependent fashion. RAW 264.7 cells were incubated with 20 ng/mL LPS and varying concentrations of **103** for 20 h. Data is shown with ligand-induced cells normalized to a fold change of 1. Treatment with **103** decreases iNOS mRNA up to 67%. Data shown is the average quantification of three biological replicates, each in technical duplicate, with error bars represented as the standard deviation. \*\*  $p \leq 0.01$ , \*\*\*\*  $p \leq 0.0001$ .

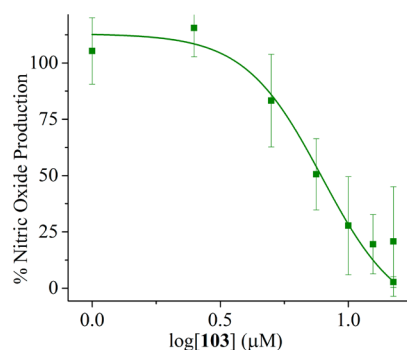
required to target the specific site of action for **103**. Taken together, our results provide consistent evidence that **103** functions through the interferon-induced JAK/STAT1 signaling pathway, suppressing iNOS.

## CONCLUSIONS

In summary, we report the identification of a group of novel IFN inhibitors based on a saccharine core. Extensive SAR studies have shown a narrow tolerance for change at the lone amido position. A Boc protected furfurylamide has proven to be the most consistently successful substituent. Our results demonstrate that **103** is a potent inhibitor of iNOS on both an mRNA and protein expression level. However, this occurs without NF- $\kappa$ B modulation, indicating a TLR-independent mechanism. Further biochemical studies imply potential inhibition in the STAT1 pathway, as this is shared between type I and II interferons, and associated genes were observed to



**Figure 4.** (A) **103** treatment reduces iNOS protein expression in a dose-dependent fashion. The iNOS protein is induced by LPS treatment and decreases with compound treatment, suggesting that compound reduces the inflammation that results in iNOS expression. The image shown is a representative image, with brightness and contrast adjusted for clarity. (B) Quantification of iNOS Western blot. Data was normalized to GAPDH as a loading control. Data shown is the average quantification of three biological replicates, with error bars represented as the standard deviation. \*\*\*  $p \leq 0.001$ .



**Figure 5.** **103** inhibits IFN- $\gamma$  signaling in a dose-dependent fashion. RAW 264.7 cells were treated with 5 ng/mL IFN- $\gamma$  to activate JAK/STAT1 signaling. Treatment with **103** decreased NO production in a dose-dependent fashion. These results suggest that **103** inhibits NO through the JAK/STAT1 pathway. Data was normalized [(raw data-untreated cells)/(TLR agonist + solvent control-untreated cells)] such that TLR ligand + solvent is 100% activation, and untreated cells are 0% activation. Data points shown are the average of nine replicates, with error bars represented as the standard deviation.

change via PCR array. **103** may provide therapeutic insight for inflammatory diseases such as systemic lupus erythematosus and multiple sclerosis.

## ASSOCIATED CONTENT

### Supporting Information

General chemistry information, synthetic methods, compound characterization, and cell-based assay data. This material is available free of charge via the Internet at <http://pubs.acs.org>.

## AUTHOR INFORMATION

### Corresponding Author

\*Phone: +1-303-492-6786. E-mail: hubert.yin@colorado.edu.

### Author Contributions

†A.C. and C.S. contributed equally to this work.

### Notes

The authors declare no competing financial interest.

## ACKNOWLEDGMENTS

We thank the National Institutes of Health (grants GM101279 and GM103843) for financial support. We thank Noah Kastelowitz for critical reading of the manuscript and assistance with statistical calculations.

## ABBREVIATIONS USED

NO, nitric oxide; IFN, interferon; JAK, Janus kinase; STAT, signal transduction and activator of transcription; iNOS, inducible nitric oxide synthase; TLR, Toll-like receptor; LPS, lipopolysaccharide; NF- $\kappa$ B, nuclear factor  $\kappa$  B; IFNAR1, interferon- $\alpha/\beta$  receptor 1; NFGFR, interferon- $\gamma$  receptor; SEAP, secreted embryonic alkaline phosphatase; TNF- $\alpha$ , tumor necrosis factor- $\alpha$ ; TNFR, tumor necrosis factor receptor; RT-PCR, real-time polymerase chain reaction; ELISA, enzyme-linked immunosorbent assay

## REFERENCES

- (1) Schroder, K.; Hertzog, P.; Ravasi, T.; Hume, D. Interferon- $\Gamma$ : An Overview of Signals, Mechanisms and Functions. *J. Leukococyte Biol.* **2004**, *75*, 163–189.
- (2) Schindler, C.; Levy, D. E.; Decker, T. JAK-STAT Signaling: From Interferons to Cytokines. *J. Biol. Chem.* **2007**, *282*, 20059–20063.
- (3) Kota, R. S.; Rutledge, J. C.; Gohil, K.; Kumar, A.; Enelow, R. I.; Ramana, C. V. Regulation of Gene Expression in RAW 264.7 Macrophage Cell Line by Interferon-Gamma. *Biochem. Biophys. Res. Commun.* **2006**, *342*, 1137–1146.
- (4) Takeda, K.; Akira, S. TLR Signaling Pathways. *Semin. Immunol.* **2004**, *16*, 3–9.
- (5) Buchanan, M. M.; Hutchinson, M.; Watkins, L. R.; Yin, H. Toll-like Receptor 4 in CNS Pathologies. *J. Neurochem.* **2010**, *114*, 13–27.
- (6) Schroder, K.; Sweet, M. J.; Hume, D. A. Signal Integration between IFN $\gamma$  and TLR Signaling Pathways in Macrophages. *Immunobiology* **2006**, *211*, 511–524.
- (7) Lowenstein, C.; Alley, E.; Raval, P.; Snowman, A.; Snyder, S.; Russell, S.; Murphy, W. Macrophage Nitric Oxide Synthase Gene: Two Upstream Regions Mediate Induction by Interferon Gamma and Lipopolysaccharide. *Proc. Natl. Acad. Sci. U. S. A.* **1993**, *90*, 9730–9734.
- (8) Gessani, S.; Belardelli, F.; Pecorelli, A.; Puddu, P.; Baglioni, C. Bacterial Lipopolysaccharide and Gamma Interferon Induce Transcription of Beta Interferon mRNA and Interferon Secretion in Murine Macrophages. *J. Virol.* **1989**, *63*, 2785–2789.
- (9) Jacobs, A.; Ignarro, L. J. Lipopolysaccharide-Induced Expression of Interferon-Beta Mediates the Timing of Inducible Nitric-Oxide Synthase Induction in RAW 264.7 Macrophages. *J. Biol. Chem.* **2001**, *276*, 47950–47957.
- (10) Vadiveloo, P. K.; Vairo, G.; Hertzog, P.; Kola, I.; Hamilton, J. A. Role of Type I Interferons during Macrophage Activation by Lipopolysaccharide. *Cytokine* **2000**, *12*, 1639–1646.
- (11) Aktan, F. iNOS-Mediated Nitric Oxide Production and Its Regulation. *Life Sci.* **2004**, *75*, 639–653.
- (12) Santiago-Raber, M.-L.; Baccala, R.; Haraldsson, K. M.; Choubey, D.; Stewart, T. A.; Kono, D. H.; Theofilopoulos, A. N. Type-I Interferon Receptor Deficiency Reduces Lupus-like Disease in NZB Mice. *J. Exp. Med.* **2003**, *197*, 777–788.

(13) Panitch, H. S.; Hirsch, R. L.; Schindler, J.; Johnson, K. P. Treatment of Multiple Sclerosis with Gamma Interferon: Exacerbations Associated with Activation of the Immune System. *Neurology* **1987**, *37*, 1097–1102.

(14) Baccala, R.; Hoebe, K.; Kono, D. H.; Beutler, B.; Theofilopoulos, A. N. TLR-Dependent and TLR-Independent Pathways of Type I Interferon Induction in Systemic Autoimmunity. *Nature Med.* **2007**, *13*, 543–551.

(15) Lio, D.; Scola, L.; Crivello, A.; Bonafè, M.; Franceschi, C.; Olivieri, F.; Colonna-Romano, G.; Candore, G.; Caruso, C. Allele Frequencies of +874T—A Single Nucleotide Polymorphism at the First Intron of Interferon-Gamma Gene in a Group of Italian Centenarians. *Exp. Gerontol.* **2002**, *37*, 315–319.

(16) Colorado Center for Drug Discovery; www.c2d2.org.

(17) Lewis, S.; Miller, G.; Hausman, M.; Szamborski, E. Isothiazoles I: 4-Isothiazolin-3-Ones. A General Synthesis from 3,3'-Dithiodipropionamides. *J. Heterocycl. Chem.* **1971**, *8*, 571–580.

(18) Combs, A. P.; Yue, E. W.; Bower, M.; Ala, P. J.; Wayland, B.; Douty, B.; Takvorian, A.; Polam, P.; Wasserman, Z.; Zhu, W.; Crawley, M. L.; Pruitt, J.; Sparks, R.; Glass, B.; Modi, D.; McLaughlin, E.; Bostrom, L.; Li, M.; Galya, L.; Blom, K.; Hillman, M.; Gonville, L.; Reid, B. G.; Wei, M.; Becker-Pasha, M.; Klabe, R.; Huber, R.; Li, Y.; Hollis, G.; Burn, T. C.; Wynn, R.; Liu, P.; Metcalf, B. Structure-Based Design and Discovery of Protein Tyrosine Phosphatase Inhibitors Incorporating Novel Isothiazolidinone Heterocyclic Phosphotyrosine Mimetics. *J. Med. Chem.* **2005**, *48*, 6544–6548.

(19) Porter, N. A.; Carter, R. L.; Mero, C. L.; Roepel, M. G.; Curran, D. P. Penultimate Group Effects in Free Radical Telomerizations of Acrylamides. *Tetrahedron* **1996**, *52*, 4181–4198.

(20) Vidal, J. A. G.; Seglar, J. F. D.; Chavez, M. T. Derivatives of Benzo[d]isothiazoles as Histones Deacetylase Inhibitors. US20090312377 A1, 2009.

(21) Samson, S. I.; Richard, O.; Tavian, M.; Ranson, T.; Vosshenrich, C. A. J.; Colucci, F.; Buer, J.; Grosveld, F.; Godin, I.; Di Santo, J. P. GATA-3 Promotes Maturation, IFN-Gamma Production, and Liver-Specific Homing of NK Cells. *Immunity* **2003**, *19*, 701–711.

(22) Elser, B.; Lohoff, M.; Kock, S.; Giaisi, M.; Kirchhoff, S.; Krammer, P. H.; Li-Weber, M. IFN-Gamma Represses IL-4 Expression via IRF-1 and IRF-2. *Immunity* **2002**, *17*, 703–712.